



**HAL**  
open science

## Modeling the trajectory of a microparticle in a dielectrophoresis device.

Mohamed Kharboutly, Michaël Gauthier, Nicolas Chaillet

► **To cite this version:**

Mohamed Kharboutly, Michaël Gauthier, Nicolas Chaillet. Modeling the trajectory of a microparticle in a dielectrophoresis device.. *Journal of Applied Physics*, 2009, 106 (11), pp.1-7. 10.1063/1.3257167 . hal-00524710

**HAL Id: hal-00524710**

**<https://hal.science/hal-00524710>**

Submitted on 8 Oct 2010

**HAL** is a multi-disciplinary open access archive for the deposit and dissemination of scientific research documents, whether they are published or not. The documents may come from teaching and research institutions in France or abroad, or from public or private research centers.

L'archive ouverte pluridisciplinaire **HAL**, est destinée au dépôt et à la diffusion de documents scientifiques de niveau recherche, publiés ou non, émanant des établissements d'enseignement et de recherche français ou étrangers, des laboratoires publics ou privés.

# Modeling the trajectory of a micro particle in a dielectrophoresis device.

Mohamed Kharboutly, Michaël Gauthier, and Nicolas Chaillet

*FEMTO-ST institute UMR CNRS 6174-UFC/ENSMM/UTBM*

*Automatic control and Micromechatronic System Department.*

*(24 rue Alain Savary, 25000 Besançon France.)*

Micro and nano-particles can be trapped by a non uniform electric field through the effect of dielectrophoretic principle. Dielectrophoresis (DEP) is used to separate, manipulate and detect micro particles in several domains, such as in biological or Carbon Nano-Tubes (CNTs) manipulations. Current methods to simulate the trajectory of micro-particles under a DEP force field are based on Finite element model (FEM) which requires new simulations when the electrode potential is changed, or on analytic equations which is limited to very simple geometries. In this paper, we propose a hybrid method between analytic and numeric calculation able to simulate complex geometries and to easily change the electrode potential along the trajectory. A few FEM simulations are used to create a database which enables online calculation of the object trajectory in function of the electrode potentials.

## I. INTRODUCTION

Dielectrophoresis force (DEP force) is the force induced on a polarizable particle suspended in a non uniform electric field. Based on the analysis of the dielectrophoretic behavior of particles, it has been demonstrated that DEP is an effective means for micro-manipulation, deposition and micro assembly [1, 2]. In modern microfluidic systems, the manipulation of biological cells and particles is a crucial technique in a variety of biomedical applications such as on-chip cell counting, separation, and isolation [3–5]. To move a micro-particle using DEP force or to control its trajectory by changing the electric potential, it is necessary to know its behavior under DEP and its trajectory [6, 7]. The first current approach is based on analytic expression applied on simple planar geometries. For example, in [8–10] researchers have developed several 2D electrodes design. They studied the shape of electrodes and its influence on the experimental DEP force in a plane. Other works have performed simulations of the DEP force using finite element simulation software [11, 12] where the trajectory of the micro particles is calculated [13–18]. The non linear micro particle's behavior and

its high dependence on the electrodes geometries induce a real complexity and some difficulties to simulate the trajectory. In this paper a hybrid method is proposed to simulate the 3D behavior of micro particles under DEP force, in function of the electric potential applied on the electrodes. Indeed, because of the large variety of electrodes and their geometric complexity, it could be highly difficult to directly integrate analytic equations. This method is based on merging preprocessed FEM simulations and analytic equations. Physicals equations are computed in order to define the link between the electric potential and the DEP force. Consequently, based on the database built by few FEM simulations, our simulator is able to provide the trajectory whatever are the electric potentials applied on the electrodes. This approach enables to improve the simulation's time. Each iteration consists of the use of the equations linking the electric potential to the electric field and then to the DEP force. FEM software can simulate complex geometries but the simulation time remains high and specially when the potential change frequently. By using FEM simulator as a preprocessing simulation and integrating physical law in a specific simulator, the time of simulation can be highly reduced. In the second section, methods able to calculate the electric field in function of the electric potential applied on the electrodes are discussed and one of them is chosen. In the third section the principle of the dynamic model is presented and in the fourth section, an experimental simulations are shown and discussed.

## II. CONCEPT OF HYBRID SIMULATION

### A. General principle

The general expression of the dielectrophoretic force applied to a micro object considered as a punctual point [19, 20] is:

$$\overrightarrow{F_{DEP}} = 2\pi\epsilon_0\epsilon_p r^3 \text{Re}[K(\omega)] \overrightarrow{\nabla E^2}, \quad (1)$$

where  $K(\omega)$  is the Clausius - Mossotti factor:

$$K(\omega) = \frac{\epsilon_p^* - \epsilon_m^*}{\epsilon_p^* + 2\epsilon_m^*}, \quad (2)$$

and

$$\epsilon^* = \epsilon + \frac{\sigma}{j\omega}, \quad (3)$$

where  $\epsilon$  are the permittivities,  $\sigma$  are the conductivities, index  $\theta$  refers to the vacuum, index  $m$  refers to the medium and index  $p$  refers to the micro object,  $r$  is the radius of the bead,  $\omega$  is the angular frequency of the applied electric field,  $\vec{\nabla}$  is the gradient operator and  $\mathbb{E}$  is the root mean square magnitude of the sinusoidal electric field. This paper focuses on the simulation of the trajectory of a spherical object in a non phased sinusoidal electric field where the DEP torque can be neglected. The DEP force is thus function of the magnitude of the electric field  $\vec{\mathbb{E}}$ , and of the frequency  $\omega$  of the electric field which modifies the value of the Clausius - Mossotti factor (2). The first challenge is to determine the spatial electric field  $\vec{\mathbb{E}}$  according to the potentials applied on the electrodes. Let us consider the magnitude of the sinusoidal electric potentials applied on  $n+1$  electrodes:

$$[\vartheta_0, \vartheta_1, \dots, \vartheta_n]. \quad (4)$$

The 3D calculation of the electric field  $\vec{\mathbb{E}}$  with respect to the potentials (4) is quite complex. Analytic calculations is in the general case not possible because of its too high complexity. To get over this difficulty we use numeric simulations. The proposed idea consists in simulating the 3D behavior of micro beads under DEP force with the minimum of numeric simulations. Firstly, we consider  $n$  potential differences:

$$U = [U_1 = \vartheta_1 - \vartheta_0, \dots, U_n = \vartheta_n - \vartheta_0]. \quad (5)$$

The first goal is to find the relation between the electric field  $\vec{\mathbb{E}}$  in a point  $M(x, y, z)$  and the potential difference  $U$  applied on these electrodes. This relation can be written as follows:

$$\vec{\mathbb{E}}(x, y, z) = \vec{f}_E(U). \quad (6)$$

## B. Numerical implementation

Different methods to numerically calculate the electric field are proposed in the following.

### 1. tridimensional space meshing

The first way to obtain a numerical expression of (6) consists in meshing the tridimensional space where the object is moving (see figure 1). Thus the objective of the algorithm is to calculate the

matrix  $E$  of the electric field:

$$E_{i,j,k,l}, \quad (7)$$

where  $i \in \{x, y, z\}$ ,  $j \in \{1, 2, \dots, n_x\}$ ,  $k \in \{1, 2, \dots, n_y\}$ , and  $l \in \{1, 2, \dots, n_z\}$ .  $n_x$ ,  $n_y$  and  $n_z$  are the number of the elementary points along  $x$ ,  $y$  and  $z$  in the meshed space.  $E_{i,j,k,l}$  represents the  $i$ th component of the electric field in the point  $M(j, k, l)$ . Two methods able to calculate (7) are discussed. Firstly the superposition theorem can be applied on the electric field. The electric field in the point  $M(j, k, l)$ , is thus a linear function of the contribution of the  $n$  potential differences  $U_m$ :

$$E_{i,j,k,l} = \sum_{m=1}^n K_{i,j,k,l,m}^E \cdot U_m \quad (8)$$

Secondly, the superposition principle can be applied on the electric potential  $\vartheta_{j,k,l}$  in the point  $M(j, k, l)$  out of electrodes:

$$\begin{aligned} E_{i,j,k,l} &= \frac{\delta}{\delta i} \vartheta_{j,k,l} \\ &= \frac{\delta}{\delta i} \sum_{m=1}^n K_{j,k,l,m}^U \cdot U_m \end{aligned} \quad (9)$$

Where  $K_{i,j,k,l,m}^E$  and  $K_{j,k,l,m}^U$  are matrix identified during preprocessing.

## 2. bidimensionnal electrode meshing

The second way to calculate a numerical expression of (6) consists in meshing the electrodes. In this case, the electrodes are meshed along two directions  $x$  and  $y$  using respectively  $e_x$  and  $e_y$  as the number of elementary steps through each direction (see figure 2). The electric field  $\vec{\mathbb{E}}$  is the sum of contributions of the elementary charges  $Q_{r,s}$  on the electrode surface at point  $P(r, s)$  (see figure 3).

The electric field at point  $M(x, y, z)$  is thus:

$$\vec{\mathbb{E}}(x, y, z) = \frac{1}{2\pi\epsilon_m} \sum_{r=1}^{e_x} \sum_{s=1}^{e_y} Q_{r,s} \cdot \frac{\overrightarrow{P(r,s)M(x,y,z)}}{\left\| \overrightarrow{P(r,s)M(x,y,z)} \right\|^3} ds, \quad (10)$$

where  $ds$  is the elementary surface on the meshed electrode.

To calculate  $Q_{r,s}$ , the superposition principle on the potential is applied:

$$Q_{r,s} = \sum_{m=1}^n C_{r,s,m} \cdot U_m. \quad (11)$$

Where  $C_{r,s,m}$  represents the elementary capacitances which can be identified during preprocessing. Thus the relation between the electric field  $\vec{\mathbb{E}}$  and the potential differences  $U$  applied on the electrodes is:

$$\vec{\mathbb{E}}(x, y, z) = \frac{1}{2\pi\epsilon_m} \sum_{r=1}^{e_x} \sum_{s=1}^{e_y} \frac{\overrightarrow{P(r, s)M(x, y, z)}}{\left\| \overrightarrow{P(r, s)M(x, y, z)} \right\|^3} \cdot \sum_{m=1}^n C_{r,s,m} \cdot U_m ds. \quad (12)$$

### 3. Discussion on the three approaches

Three numerical methods (8),(9) and (12) to calculate the electric field vector have been presented. Each method is discussed below:

1. The  $K_{i,j,k,l,m}^E$  matrix contains the necessary value to calculate the component of the electric field vector in each point of the workspace created by each electrode. The number of elements in this matrix is:

$$3 \times n_x \times n_y \times n_z \times n.$$

These parameters are calculated using 3D simulation in a limited area in the workspace.

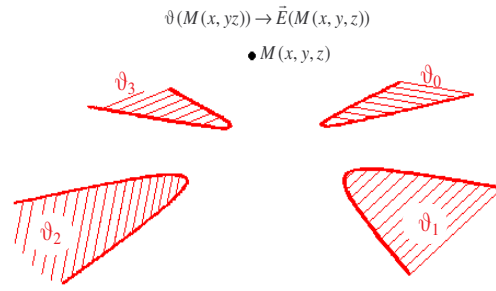
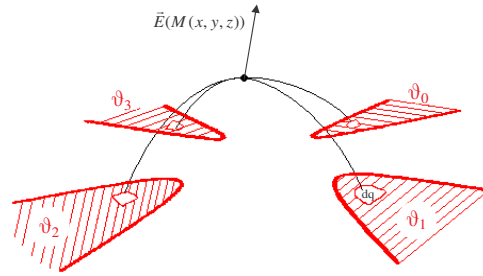
2. The  $K_{j,k,l,m}^U$  matrix contains the necessary value to calculate the spatial electric potential in each point in the workspace created by each electrode. The number of elements in this matrix is:

$$n_x \times n_y \times n_z \times n.$$

These parameters are calculated using 3D simulation in a limited area in the workspace (see in figure 1). This method requires to applied a differential operator on the numeric data (9), which could induce errors.

3. The  $C_{r,s,m}$  matrix contains the elementary capacitances created by each potential difference. The electrodes are meshed into 2D ( $e_x, e_y$ ) elementary points on the surface of each electrodes. The number of elements in this matrix is:

$$e_x \times e_y \times n.$$

FIG. 1: Calculating  $\mathbb{E}$  from the 3D electric potentialFIG. 2: Calculating  $\mathbb{E}$  for the 2D charge density

These parameters are calculated using 2D simulation and the equation (12) allows calculating the electric field vector  $\vec{\mathbb{E}}$  in any point  $M(x, y, z)$  in the workspace (see figure 2 and 3). Using this method requires the use of a double numerical integral.

Based on this comparison, it appears that the third method is more interesting. Indeed it requires a less preprocessing on 2D data and it permits calculating the electric field in any points in the space. This method is then detailed below.

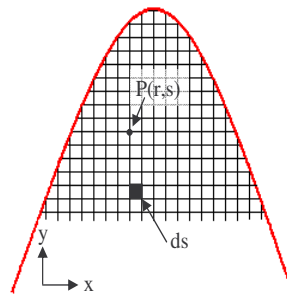


FIG. 3: Elementary charges in each electrode

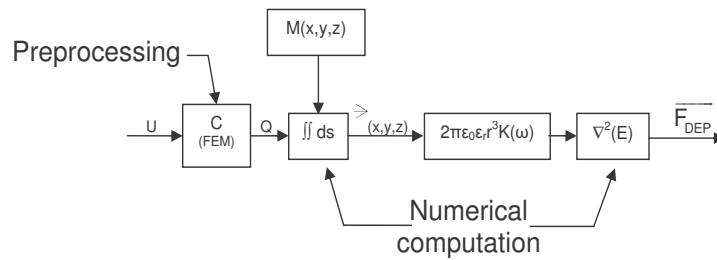


FIG. 4: Block diagram representing the link between the electric potential  $U$  and the DEP force

### C. Preprocessing

The capacitance matrix  $C$  defined in (11) is constant and is independent from the electric potential  $U$  and the charge density  $Q$ . To identify this matrix,  $n$  FEM simulations of the charge density on the electrodes in function of  $n$  algebraically independent vectors  $U$  are needed. Once the matrix  $C$  is calculated the relation between the electric field  $\vec{\mathbb{E}}$  and the electric potential  $U$  is obtained through equation (12).

### D. Static force model

The diagram presented in the figure 4 shows the procedure to calculate the DEP force in function of the potential difference  $U$ . During preprocessing, geometries, boundaries conditions and surroundings properties are specified in a FEM software and  $n$  simulations are launched. All data are arranged to create the capacitance matrix  $C$ . The link between the electric potential  $U$  and the electric field  $\vec{\mathbb{E}}$  is then calculated: the calculation of the electric field  $\vec{\mathbb{E}}$ , at the point  $M(x, y, z)$  of the micro object is possible using (12). Thus the DEP force  $\overrightarrow{F_{DEP}}$  applied to the micro object can be obtained by using (1). The frequency  $\omega$  of the electric field can also be modified during the trajectory simulation.

## III. DYNAMIC TRAJECTORY MODELING

Let us consider a micro particle immersed in a liquid medium with viscosity  $\mu$ , with a non uniform electric field created by applying electric potential on the electrodes. The forces applied on this



particle are  $\overrightarrow{F_{DEP}}$ , its own weight  $\overrightarrow{P}$  and the Stokes drag force  $\overrightarrow{F_{drag}}$  which verifies:

$$\overrightarrow{F_{drag}} = -6\pi\mu r \overrightarrow{V} = -k_\mu \overrightarrow{V} \quad (13)$$

where  $\overrightarrow{V}$  is the velocity of the particle. Using Newton's second law the particle's motion is defined by:

$$\overrightarrow{F_{DEP}} + \overrightarrow{P} - k_\mu \overrightarrow{V} = m \overrightarrow{a} \quad (14)$$

where  $m$  is the mass of the particles and  $\overrightarrow{a}$  is the acceleration vector. In order to simulate this trajectory model, an hypothesis is proposed to simplify the calculation of the position of the micro particles: The dynamic expression  $m \overrightarrow{a}$  can be neglected compared the forces. To verify this hypothesis, a study is proposed on the inertia impact on the trajectory in first subsection. Despite the fact that the weight is a volumic effect it can not be neglected. Indeed the equilibrium state is characterized by  $\overrightarrow{F_{DEP}} = \overrightarrow{P}$ , and without considering the weight, the equilibrium position is always  $z \sim \infty$ . But, in fact, the micro particle stands on a finite and stable position.

#### A. The inertia impact

To illustrate the impact of the inertia on the trajectory, a simple example of 2 punctual electrodes is presented in the figure 5 where the calculation of the electric field can be done analytically in function of the electric potential. An electric sinusoidal signal which its magnitude is  $U_0$  and frequency is  $\omega$  is applied between the punctual electrodes. The electric field on each point of the  $z$  axis is equal to:

$$\overrightarrow{E_0} = \frac{U_0 d^2}{8z^3} \overrightarrow{z}. \quad (15)$$

Using (1), DEP force can be obtained:

$$\overrightarrow{F_{DEP}} = \frac{k_{DEP} U_0^2 d^4}{z^7} \overrightarrow{z} \quad (16)$$

with

$$k_{DEP} = -\frac{3\pi\epsilon_0\epsilon_p r^3 K(\omega)}{16}. \quad (17)$$

The motion of the micro particle along  $z$  is then described by:

$$m\ddot{z} = -k_\mu \dot{z} - mg + \frac{k_{DEP} U_0^2 d^4}{z^7}. \quad (18)$$

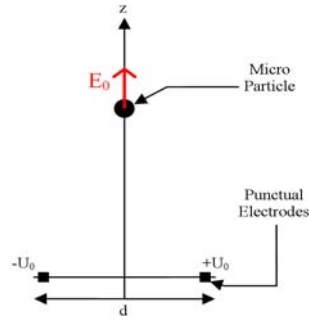


FIG. 5: Elementary electrodes used to calculate analytically the electric field with respect to the electric potential

When the micro particle reaches the equilibrium point  $z_0$  it means that the  $\overrightarrow{F_{DEP}}$  is equal to the weight:

$$z_0 = \left( \frac{k_{DEP} U_0^2 d^4}{mg} \right)^{1/7}. \quad (19)$$

By linearizing the relation (18) around  $z_0$  and using Laplace transformation we obtain:

$$\frac{z(p)}{z_0(p)} = \frac{k}{mp^2 + k_\mu p + k}, \quad (20)$$

where

$$k = 7 \frac{mg}{z_0}. \quad (21)$$

As the damping factor  $\xi$  is high, both poles  $p_1$  and  $p_2$  of the system are real and:

$$\frac{p_2}{p_1} = \frac{-\xi - (\xi^2 - 1)^{1/2}}{-\xi + (\xi^2 - 1)^{1/2}}, \quad (22)$$

where

$$\xi = \frac{k_\mu}{2k} \sqrt{\frac{k}{m}}. \quad (23)$$

To estimate the impact of both poles  $p_1$  and  $p_2$  on the trajectory, we consider a typical example: an object in polystyrene,  $\epsilon_p = 2.4$  with a radius  $r = 10\mu m$ , immersed in the water with  $\epsilon_m = 80$  and distance  $d$  of  $100\mu m$  under  $U_0 = 100V$ . The damping factor  $\xi$  reaches  $14$ . Thus:

$$\xi^2 \gg 1 \Leftrightarrow p_1 \ll p_2. \quad (24)$$

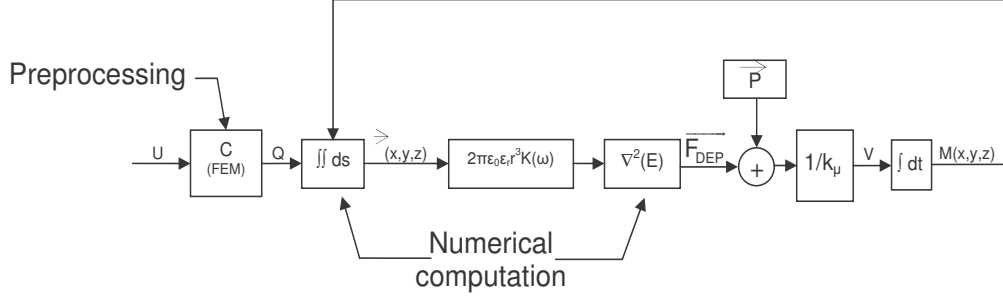


FIG. 6: Block diagram representing the dynamic modeling of a bead under DEP force

So the dynamic behavior is directly function of the predominant pole  $p_1$  and the second pole  $p_2$  can be neglected:

$$\frac{z(p)}{z_0(p)} \cong \frac{k}{k_\mu p + k}. \quad (25)$$

This dynamical equation is similar to (20) where the dynamic term  $mp^2$  has been neglected. In the proposed example, the impact of the inertia on the behavior of the micro particles can be neglected. Moreover,  $\xi$  defined in (23) is inversely proportional to the distance unit. Thus, when the dimension of the micro particle and electrodes is reduced by 10, the parameter  $\xi$  is multiplied by 10. Consequently, in micro scales  $\xi$  is typically high and the criterion (24) is typically verified. Thus we consider that the inertia impact is negligible on the trajectory of a micro particle moved by dielectrophoresis force.

### B. Dynamic model

As the inertia can be neglected, the equation (13) gives the velocity of the micro particle along the trajectory:

$$\vec{V} = \frac{(\vec{F}_{DEP} + \vec{P})}{k_\mu}. \quad (26)$$

In the figure 6, a block diagram is presented to illustrate each part of the system acting between the electric potential  $U$ , the DEP force and the micro particle's position. An applied potential difference  $U$  on the electrodes creates the non uniform electric field  $\vec{E}$  which creates the DEP force used to manipulate the micro particle. The equation (26) manages the dynamical behavior of the micro

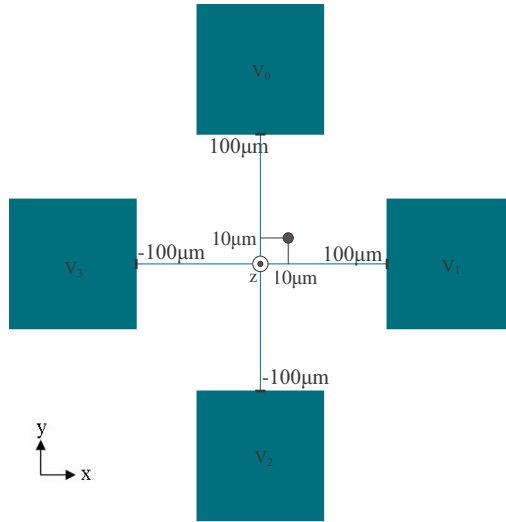


FIG. 7: Geometry of 4 electrodes used to experiment the DEP force and the initial position of the micro particle in simulation

particle under DEP force.

#### IV. EXPERIMENTAL SIMULATIONS

##### A. Trajectory of a point-shaped object

Considering the geometry of the electrodes described in the figure 7, 4 electrodes and 3 potential differences are being used. After 3 simulations under the FEM software COMSOL, the matrix  $C$  is identified as described below, and the simulator is launched. For a silicon bead of radius equal to  $50\mu\text{m}$ , submerged in the water, its motion under DEP is simulated from an initial position  $(10\mu\text{m}, -10\mu\text{m}, 55\mu\text{m})$  as it is proposed in figure 7. Applying the potential difference  $U(80\text{V}, 0\text{V}, 80\text{V})$  (5) between the electrodes using a frequency of  $40\text{KHz}$  the Clausius - Mossotti factor  $k(\omega)$  referred in (2) is equal to  $K(\omega) = -0.4252$ , the DEP force is negative and the trajectory of the bead can be predicted. In the simulated trajectory, there is no presence of the equilibrium state along the axis  $z$  (see figure 9). In the first phase of the motion, the bead goes up when it moves toward the axis  $z$ . After reaching the equilibrium point in the  $XY$  plane (see figure 8), the bead start the sedimentation phase and goes down. This motion is caused by the DEP force calculated, which is equal to zero on the micro particle's center. However, experiments done on this geometry,

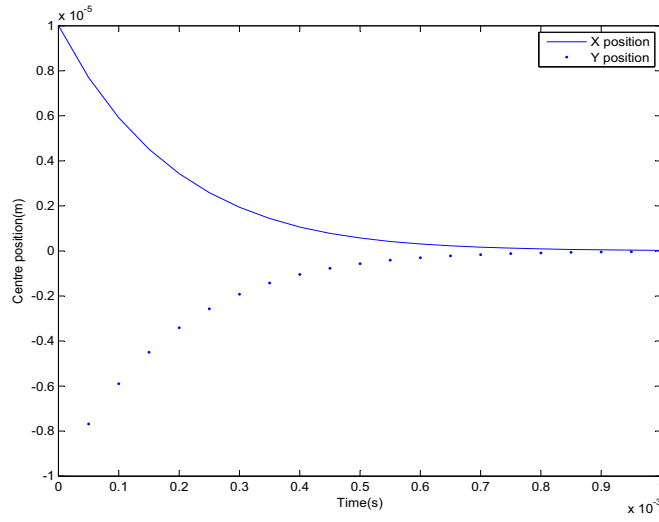


FIG. 8: x, y trajectory of the punctual micro particle under DEP force

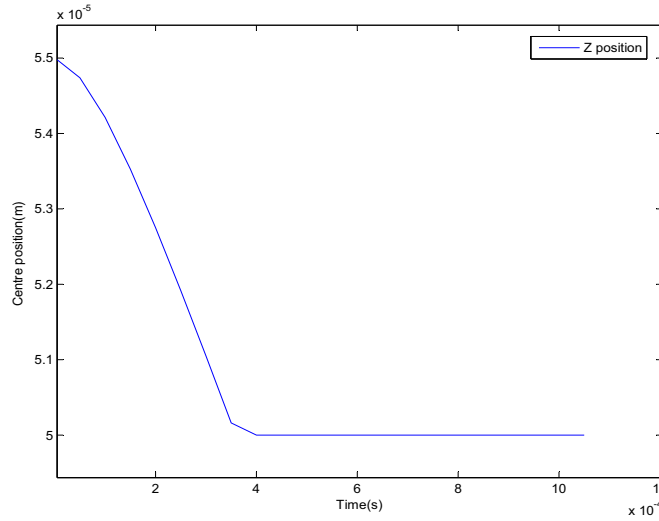


FIG. 9: z trajectory of the punctual micro particle under DEP force

using electrodes made from gold and deposit on a silicon wafer immersed in an ultra pure water and a silicon bead of radius equal to  $50\mu m$ , show that an equilibrium point exists in the center of the electrodes (see in figure 10) along the axis  $z$  (see in figure 11). In this figure 11, the micro bead and its reflexion on the wafer are shown on a lateral view. In the left view, the micro bead is on the wafer when an electric potential of  $U(60V, 0V, 60V)$  is applied. In this case, the  $z$  component of the DEP force is smaller than the weight of the micro bead. In the right view, the micro bead is in levitation above the electrodes plane when an electric potential of  $U(80V, 0V, 80V)$  is applied. This difference between the experimental results and the simulated result appear because the hypothesis used in

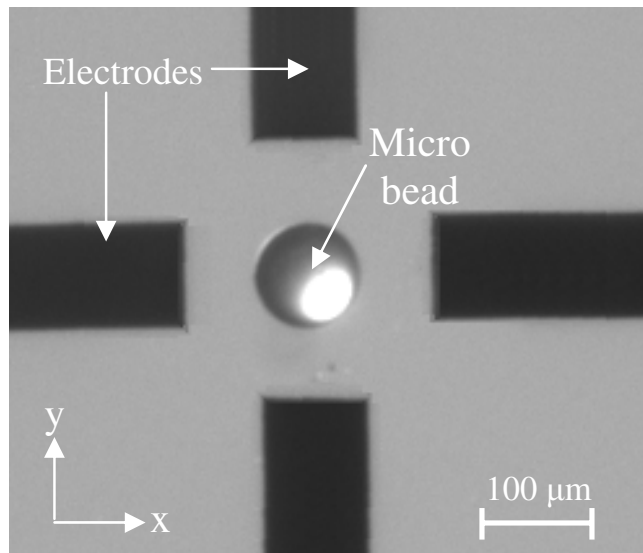


FIG. 10: Vertical view: Electrodes used in the experiments. The micro particle is in the center of electrodes. The applied tension is  $U(80V, 0V, 80V)$

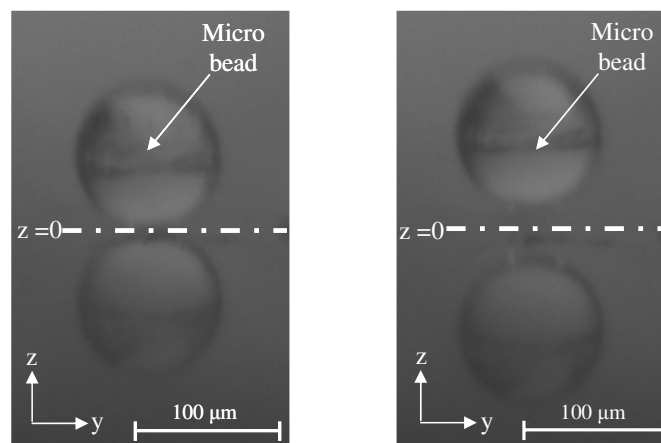


FIG. 11: Lateral view: The micro bead is in direct contact with the electrodes plane (Left view) when applying a tension of  $U(60V, 0V, 60V)$ . The micro particle is in levitation up to the electrodes (Right view) when applying a tension of  $U(80V, 0V, 80V)$ .

(1) (micro particle is considered as a punctual point) is not available in the equilibrium point. This hypothesis induces a zero DEP force while the real force is not zero.

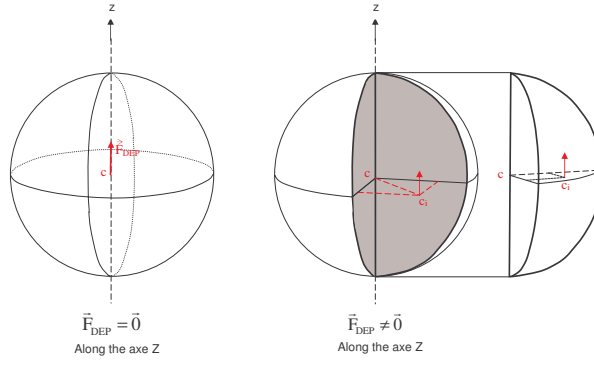


FIG. 12: Use of the punctual bead (left), use of the volumic particle(right). Only  $z$  component of the electric field is presented

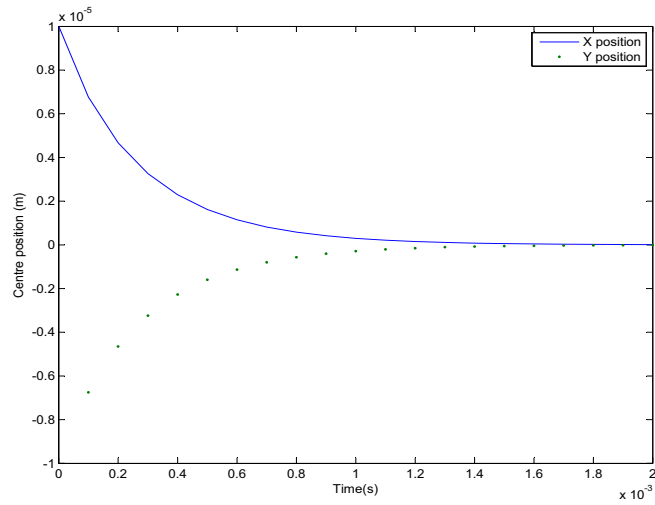


FIG. 13:  $x$ ,  $y$  trajectory of the volumic particle under DEP force

### B. Trajectory of a volume object

To solve this problem, the micro particle is divided into 4 identical parts around its vertical axes and then all forces applied on each part are calculated to find the general force by summing all forces together (see figure 12). Figures 13 and 14 show the trajectory of the micro particle using the same initial conditions as above. Using this method, the simulated trajectory of the micro particle convinces more with the real trajectory and the simulation results show that the micro particle reaches an equilibrium point as observed in the experimental results.

Using our simulator, non linear trajectories can be simulated. Multi initials positions of a micro bead of radius equal to  $10\mu m$ , under the same potential ( $U = 80V$ ), could be simulated and the

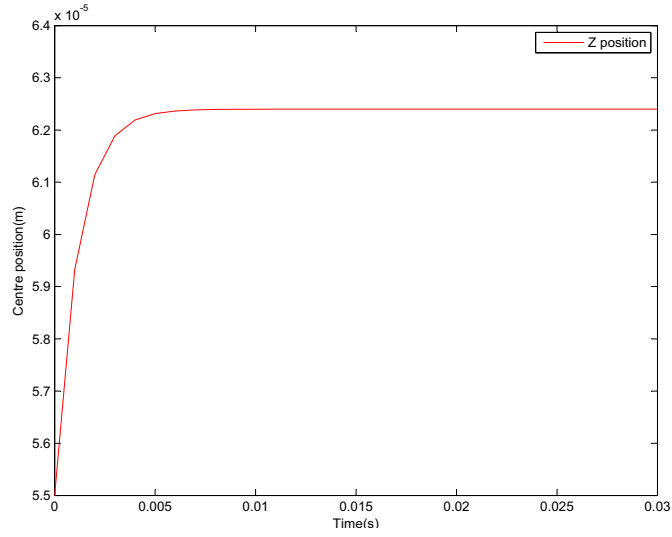


FIG. 14: z trajectory of the volumic particle under DEP force

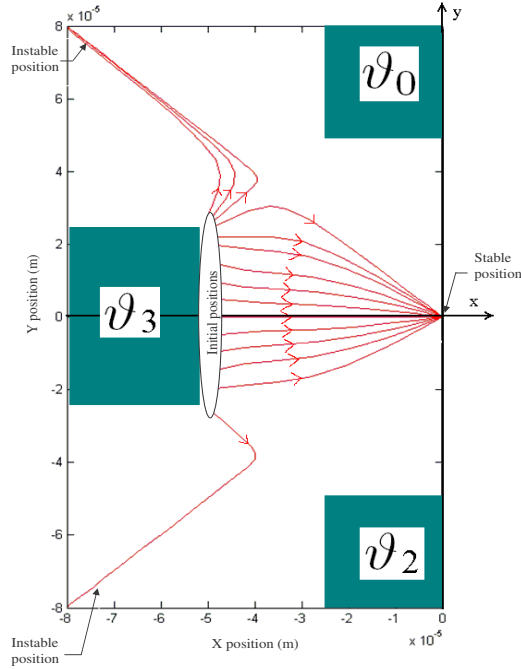


FIG. 15: Projection of non linear simulated trajectories in the  $(x,y)$  plane

projection on  $xy$  plane of the resulted trajectories are presented in figure 15.

## V. DISCUSSION

Using a calculator with relatively high performance (Intel Xeon CPU 1.60 GHz (2 CPUs) with 3 GB of RAM) the measured time to simulate the electric field and calculate the DEP force applied



on a particle using the electrodes described in figure 10 and its trajectory under the FEM software COMSOL 3.5 is 2 minutes.

Using the same calculator to simulate the charge density on the electrodes is 30 seconds. To create the base used in our simulator we need 3 FEM simulations witch means 1 minute 30 seconds.

Using this database, the time needed to calculate the trajectory is 10 seconds.

Thus comparing both methods, the time needed to simulate  $n$  trajectories of a micro object by applying  $n$  different tensions on the electrodes is:

1. For the FEM software:  $2 \times n$  minutes.
2. For our simulator: 1 minute 30 seconds +  $11 \times n$  seconds.

Consequently, our approach, based on the use of FEM as a preprocessing, enables to clearly reduce the time of computation especially when different values of tension  $U$  have to be simulated on the same geometry. Moreover, in this simulator, the calculated electric field is not limited in the space, it can be calculated in any point in the space contrarily to the FEM software, where the space is meshed. Moreover this simulator does not take into account the DEP torque, but the general principle proposed here can be extended to angular positioning. This aspect will be explored in future works.

## VI. CONCLUSION

We have proposed a new model and simulator using a hybrid method in which we combined both analytic and numeric calculation to simulate the behavior of a micro bead (spherical object) under DEP force. A pre-simulation under FEM software allows to obtain a database with respect to the electrode geometries. Based on the preprocessing, the simulator integrates the dynamical behavior equation to simulate the electric field under different tensions applied on the electrodes. An example of 4 electrodes have been discussed and compared to experiments. Current works are focused on the use of this model to study control laws able to move the micro particle along a specified trajectory.

## VII. ACKNOWLEDGMENTS

This work is supported by the French research projects PRONOMIA N: ANR 05 – *BLAN* – 0325 – 01 and NANOROL N: ANR 07 – *ROBO* – 0003 – 01.

- 
- [1] Gauthier M., Gibeau E., and Heriban D. Submerged robotic micromanipulation and dielectrophoretic micro-object release. In *Control, Automation, Robotics and Vision, 2006. ICARCV 9th International Conference*, pages 1–6, 2006.
- [2] M. Gauthier, S. Regnier, P. Rougeot, and N. Chaillet. Analysis of forces for micromanipulations in dry and liquid media. *Journal of Micromechatronics*, 3(3-4):389413, 2006.
- [3] K. Hyoungh Kang, X. Xuan, Y. Kang, and D. Li. Effects of dc-dielectrophoretic force on particle trajectories in microchannels. *Journal of Applied Physics*, 99:064702, 2006.
- [4] K. M. Slenes, P. Winsor, T. Scholz, and M. Hudis. Pulse power capability of high energy density capacitors based on a new dielectric material. *IEEE Trans. Magn.*, 37:324, 2001.
- [5] M. E. Staben and R. H. Davis. Particle transport in poiseuille flow in narrow channels. *Int. J. Multiphase Flow*, 31:529, 2005.
- [6] M. Dimaki and P. Boggild. Dielectrophoresis of carbon nanotubes using microelectrodes: a numerical study. *Nanotechnology*, 5:1095–1102, 2004.
- [7] N. Peng, Q. Zhang, J. Li, and N. Liu. Influences of ac electric field on the spatial distribution of carbon nanotubes formed between electrodes. *JOURNAL OF APPLIED PHYSICS*, 100:024309, 2006.
- [8] V. Tomer, C. A. Randall, G. Polizos, J. Kostelnick, and E. Manias. High- and low-field dielectric characteristics of dielectrophoretically aligned ceramic/polymer nanocomposites. *Journal of Applied Physics*, 103:034115–1–7, 2008.
- [9] Wejinya, U.C., N. Xi, K. Lai, J. Zhang, and Y. Shen. Design and generation of dep force for assembly of cnt-based nano devices. In *IEE/RSJ International Conference on Intelligent Robots and Systems*, pages 925 – 929, Nice, France, Sept 2008.
- [10] C. Y. Yang and U. Lei. Quasistatic force and torque on ellipsoidal pa under generalized dielectrophoresis. *Journal of Applied Physics*, 102:094702–1–11, 2007.
- [11] A. Heeren, C.P.Luo, W. Henschel, M.Fleischer, and D.P. Kern. Manipulation of micro- and nanoparticles by electro-osmosis and dielectrophoresis. *Microelectronic Engineering*, 84:1706 – 1709, February 2007.
- [12] N. Aubry J. Kadaksham, P. Singh. Manipulation of particles using dielectrophoresis. *Mechanics Research Communications*, 33:108 – 122, july 2006.
- [13] A. Al-Jarro, J. Paul, D. W. P. Thomas, J. Crowne, and N. Sawyer. Direct calculation of maxwell stress tensor for accurate trajectory prediction during dep for 2d and 3d structures. *Journal of Physics:*

- Applied Physics*, 40:71–77, 2007.
- [14] Y. Liu, J. H. Chung, W. K. Liu, and R. S. Ruoff. Dielectrophoretic assembly of nanowires. *Journal of Physics*, 110:14098–14106, 2006.
- [15] J. Kim and C. Han. Use of dielectrophoresis in the fabrication of an atomic force microscope tip with a carbon nanotube: a numerical analysis. *Institute of Physics Publishing: Nanotechnology*, 16:2245–2250, 2005.
- [16] M. Li, Y. Qu, Z. Dong, W. J. Li, and Y. Wang. Design and simulation of electrodes for 3d dielectrophoretic trapping. In *Proceedings of the 3rd IEEE Int. Conf. on Nano/Micro Engineered and Molecular Systems*, pages 733 – 737, Sanya, China, January 2008.
- [17] M. I. P. Hughes, H. Morgan, and M. F. Flynn. The dielectrophoretic behavior of submicron latex spheres: Influence of surface conductance. *Journal of Colloid and Interface Science*, 220:454 – 457, September 1999.
- [18] Z. i. Zo, S. Lee, and C. H. Ahn. A polymer microfluidic chip with interdigitated electrodes arrays for simultaneous dielectrophoretic manipulation and impedimetric detection of microparticles. *IEEE Sensors Journal*, 8(5):527 – 535, May 2008.
- [19] F. T. Chang, Y. C. Lee, and C. C. Chiu. Multiple electrodes arrayed dielectrophoretic chip with application on micro-bead manipulation. In *Proceedings of the 3rd IEEE Int. Conf. on Nano/Micro Engineered and Molecular Systems*, pages 850 – 853, Sanya, China, January 2008.
- [20] P. R. C. Gascoyne and J. V. Vykoual. Dielectrophoresis-based sample handling in general-purpose programmable diagnostic instruments. *IEEE Sensors Journal*, 92(1):22 – 42, January 2004.
- [21] T. B. Jones. *Electromechanics of Particles*. Cambridge University Press, 1995.
- [22] H. M. and N. G. Green. *AC Electrokinetics: Colloids and Nanoparticles*. Hertfordshire: Research Studies Press, 2003.